Survival Probability of Large Rapidity Gaps

E. Gotsman, E. Levin, U. Maor, E. Naftali, A. Prygarin
HEP Department, School of Physics and Astronomy, Raymond and Beverly Sackler Faculty of Exact Science, Tel Aviv University, Tel Aviv, 69978, ISRAEL.

Abstract

Our presentation centers on the consequences of s-channel unitarity, manifested by soft re-scatterings of the spectator partons in a high energy diffractive process, focusing on the calculations of gap survival probabilities. Our emphasis is on recent estimates relevant to exclusive diffractive Higgs production at the LHC. To this end, we critically re-examine the comparison of the theoretical estimates of large rapidity gap hard di-jets with the measured data, and remark on the difficulties in the interpretation of HERA hard di-jet photoproduction.

1 Introduction

A large rapidity gap (LRG) in an hadronic, photo or DIS induced final state is experimentally defined as a large gap in the $\eta - \phi$ lego plot devoid of produced hadrons. LRG events were suggested [1–4] as a signature for Higgs production due to a virtual $W - W$ fusion subprocess. An analogous pQCD process, in which a colorless exchange ("hard Pomeron") replaces the virtual W, has a considerably larger discovery potential as it leads also to an exclusive $p + H + p$ final state. Assuming the Higgs mass to be in the range of $100 - 150 \, GeV$, the calculated rates for this channel, utilizing proton tagging are promising. Indeed, LRG hard di-jets, produced via the same production mechanism, have been observed in the Tevatron [5–17] and HERA [18–29]. The experimental LRG di-jets production rates are much smaller than the pQCD (or Regge) estimates. Following Bjorken [3, 4], the correcting damping factor is called "LRG survival probability".

The present summary aims to review and check calculations of the survival probability as applied to the HERA-Tevatron data and explore the consequences for diffractive LRG channels at LHC with a focus on diffractive Higgs production.

We distinguish between three configurations of di-jets (for details see Ref. [13–17]):

1) A LRG separates the di-jets system from the other non diffractive final state particles. On the partonic level this is a single diffraction (SD) Pomeron exchange process denoted GJJ.

2) A LRG separates between the two hard jets. This is a double diffraction (DD) denoted JGJ.

3) Centrally produced di-jets are separated by a LRG on each side of the system. This is a central diffraction (CD) two Pomeron exchange process denoted GJJG. This mechanism also leads to diffractive exclusive Higgs production.

We denote the theoretically calculated rate of a LRG channel by F_{gap}. It was noted by Bjorken [3, 4] that we have to distinguish between the theoretically calculated rate and the actual measured rate f_{gap}

$$f_{gap} = \langle | S |^2 \rangle \cdot F_{gap}. \tag{1}$$

The proportionality damping factor [30–33] is the survival probability of a LRG. It is the probability of a given LRG not to be filled by debris (partons and/or hadrons). These debris originate from the soft re-scattering of the spectator partons resulting in a survival probability denoted $| S_{spec}(s) |^2$, and/or from the gluon radiation emitted by partons taking part in the hard interaction with a corresponding survival probability denoted $| S_{brem}(\Delta y) |^2$,

$$\langle | S(s, \Delta y) |^2 \rangle = \langle | S_{spec}(s) |^2 \rangle \cdot \langle | S_{brem}(\Delta y) |^2 \rangle. \tag{2}$$

s is the c.m. energy square of the colliding particles and Δy is the large rapidity gap. Gluon radiation from the interacting partons is strongly suppressed by the Sudakov factor [34]. However, since this suppression is included in the perturbative calculation (see **4.3**) we can neglect $\langle \mid S_{brem}(\Delta y) \mid^2 \rangle$ in our calculations. In the following we denote $\langle \mid S_{spec} \mid^2 \rangle = S^2$. It is best defined in impact parameter space (see **2.1**)). Following Bjorken [3, 4], the survival probability is determined as the normalized integrated product of two quantities

$$S^2 = \frac{\int d^2b \mid M^H(s,b) \mid^2 P^S(s,b)}{\int d^2b \mid M^H(s,b) \mid^2}. \tag{3}$$

$M^H(s,b)$ is the amplitude for the LRG diffractive process (soft or hard) of interest. $P^S(s,b)$ is the probability that no inelastic soft interaction in the re-scattering eikonal chain results in inelasticity of the final state at (s,b).

The organization of this paper is as follows: In Sec.2 we briefly review the role of s-channel unitarity in high energy soft scattering and the eikonal model. The GLM model [30–33] and its consequent survival probabilities [35–37] are presented in Sec.3, including a generalization to a multi channel re-scattering model [38, 39]. The KKMR model [40–44] and its survival probabilities is presented in Sec.4. A discussion and our conclusions are presented in Sec.5. An added short presentation on Monte Carlo calculations of S^2 is given in an Appendix.

2 Unitarity

Even though soft high energy scattering has been extensively studied experimentally over the last 50 years, we do not have, as yet, a satisfactory QCD framework to calculate even the gross features of this impressive data base. This is just a reflection of our inability to execute QCD calculations in the non-perturbative regime. High energy soft scattering is, thus, commonly described by the Regge-pole model [45, 46]. The theory, motivated by S matrix approach, was introduced more than 40 years ago and was soon after followed by a very rich phenomenology.

The key ingredient of the Regge pole model is the leading Pomeron, whose linear t-dependent trajectory is given by

$$\alpha_{I\!P}(t) = \alpha_{I\!P}(0) + \alpha'_{I\!P}t. \tag{4}$$

A knowledge of $\alpha_{I\!P}(t)$ enables a calculation of σ_{tot}, σ_{el} and $\frac{d\sigma_{el}}{dt}$, whose forward elastic exponential slope is given by

$$B_{el} = 2B_0 + 2\alpha'_{I\!P}ln\left(\frac{s}{s_0}\right). \tag{5}$$

Donnachie and Landshoff (DL) have vigorously promoted [47, 48] an appealing and very simple Regge parametrization for total and forward differential elastic hadron-hadron cross sections in which they offer a global fit to all available hadron-hadron and photon-hadron total and elastic cross section data. This data, above $P_L = 10\,GeV$, is excellently fitted with universal parameters. We shall be interested only in the DL Pomeron with an intercept $\alpha_{I\!P}(0) = 1 + \epsilon$, where $\epsilon = 0.0808$, which accounts for the high energy growing cross sections. Its fitted [49] slope value is $\alpha'_{I\!P} = 0.25\,GeV^{-2}$.

2.1 S-channel unitarity

The simple DL parametrization is bound to violate s-channel unitarity at some energy since σ_{el} grows with energy as $s^{2\epsilon}$, modulu logarithmic corrections, while σ_{tot} grows only as s^ϵ. The theoretical problems at stake are easily identified in an impact b-space representation.

The elastic scattering amplitude is normalized so that

$$\frac{d\sigma_{el}}{dt} = \pi \mid f_{el}(s,t) \mid^2, \tag{6}$$

input

output

1

unitarity bound

analyticity/crossing bound

a(b,s)

b
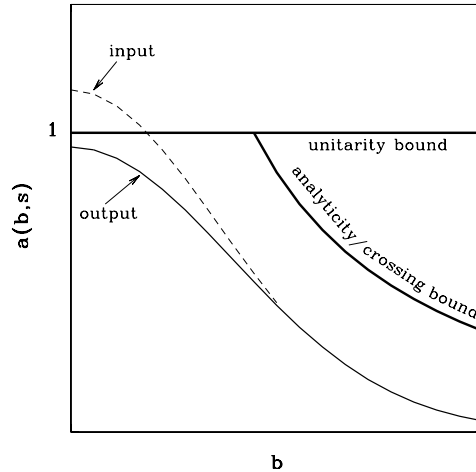
Fig. 1: A pictorial illustration of a high energy b-space elastic amplitude bounded by unitarity and analyticity/crossing. In the illustration we have an input amplitude which violates the eikonal unitarity bound and an output amplitude obtained after a unitarization procedure.

$$\sigma_{tot} = 4\pi Im f_{el}(s,0). \tag{7}$$

The elastic amplitude in b-space is defined as

$$a_{el}(s,b) = \frac{1}{2\pi} \int d\mathbf{q} e^{-i\mathbf{q}\cdot\mathbf{b}} f_{el}(s,t), \tag{8}$$

where $t = -\mathbf{q}^2$. In this representation

$$\sigma_{tot} = 2 \int d^2b \, Im[a_{el}(s,b)], \tag{9}$$

$$\sigma_{el} = \int d^2b \mid a_{el}(s,b) \mid^2, \tag{10}$$

$$\sigma_{in} = \sigma_{tot} - \sigma_{el}. \tag{11}$$

As noted, a simple Regge pole with $\alpha_{I\!P}(0) > 1$ will eventually violate s-channel unitarity. The question is if this is a future problem to be confronted only at far higher energies than presently available, or is it a phenomena which can be identified through experimental signatures observed within the available high energy data base. It is an easy exercise to check that the DL model [47, 48], with its fitted global parameters, will violate the unitarity black bound (see **2.2**) at very small b, just above the present Tevatron energy. Indeed, CDF reports [50] that $a_{el}(b = 0, \sqrt{s} = 1800) = 0.96 \pm 0.04$. A pictorial illustration of the above is presented in Fig.1. Note that the energy dependence of the experimental SD cross section [13–17] in the ISR-Tevatron energy range is much weaker than the power dependences observed for σ_{el}. Diffractive cross sections are not discussed in the DL model.

2.2 The eikonal model

The theoretical difficulties, pointed out in the previous subsection, are eliminated once we take into account the corrections necessitated by unitarity. The problem is that enforcing unitarity is a model dependent procedure. In the following we shall confine ourselves to a Glauber type eikonal model

[51]. In this approximation, the scattering matrix is diagonal and only repeated elastic re-scatterings are summed. Accordingly, we write

$$a_{el}(s,b) = i\left(1 - e^{-\Omega(s,b)/2}\right).$$ (12)

Since the scattering matrix is diagonal, the unitarity constraint is written as

$$2Im[a_{el}(s,b)] = \mid a_{el}(s,b)\mid^2 + G^{in}(s,b),$$ (13)

with

$$G^{in} = 1 - e^{-\Omega(s,b)}.$$ (14)

The eikonal expressions for the soft cross sections of interest are

$$\sigma_{tot} = 2\int d^2b\left(1 - e^{-\Omega(s,b)/2}\right),$$ (15)

$$\sigma_{el} = \int d^2b\left(1 - e^{-\Omega(s,b)/2}\right)^2,$$ (16)

$$\sigma_{in} = \int d^2b\left(1 - e^{-\Omega(s,b)}\right),$$ (17)

and

$$B_{el}(s) = \frac{\int d^2b\, b^2\left(1 - e^{-\Omega(s,b)/2}\right)}{2\int d^2b\left(1 - e^{-\Omega(s,b)/2}\right)}.$$ (18)

From Eq.(14) it follows that $P^S(s,b) = e^{-\Omega(s,b)}$ is the probability that the final state of the two initial interacting hadrons is elastic, regardless of the eikonal rescattering chain. It is identified, thus, with $P^S(s,b)$ of Eq.(3).

Following our implicit assumption that, in the high energy limit, hadrons are correct degrees of freedom, i.e. they diagonalize the interaction matrix, Eq.(12) is a general solution of Eq.(13) as long as the input opacity Ω is arbitrary. In the eikonal model Ω is real and equals the imaginary part of the iterated input Born amplitude. The eikonalized amplitude is imaginary. Its analyticity and crossing symmetry are easily restored. In a Regge language we substitute, to this end, $s^{\alpha_{I\!P}} \to s^{\alpha_{I\!P}}e^{-\frac{1}{2}i\pi\alpha_{I\!P}}$.

In the general case, Eq.(13) implies a general bound, $\mid a_{el}(s,b)\mid \le 2$, obtained when $G^{in} = 0$. This is an extreme option in which asymptotically $\sigma_{tot} = \sigma_{el}$ [52]. This is formally acceptable but not very appealing. Assuming that a_{el} is imaginary, we obtain that the unitarity bound coincides with the black disc bound, $\mid a_{el}(s,b)\mid \le 1$. Accordingly,

$$\frac{\sigma_{el}}{\sigma_{tot}} \le \frac{1}{2}.$$ (19)

3   The GLM Model

The GLM screening correction (SC) model [30–33] is an eikonal model originally conceived so as to explain the exceptionally mild energy dependence of soft diffractive cross sections. It utilized the observation that s-channel unitarization enforced by the eikonal model operates on a diffractive amplitude in a different way than it does on the elastic amplitude. The GLM diffractive damping factor is identical to Bjorken's survival probability.

3.1 The GLM SC model

In the GLM model, we take a DL type Pomeron exchange amplitude input in which $\alpha_{I\!P}(0) = 1 + \Delta > 0$. The simplicity of the GLM SC model derives from the observation that the eikonal approximation with a central Gaussian input, corresponding to an exponential slope of $\frac{d\sigma_{el}}{dt}$, can be summed analytically. This is, clearly, an over simplification, but it reproduces the bulk of the data well, i.e. the total and the forward elastic cross sections. Accordingly, the eikonal DL type b-space expression for $\Omega(s, b)$ is:

$$\Omega(s, b) = \nu(s)\,\Gamma^S(s, b), \tag{20}$$

where,

$$\nu(s) = \sigma(s_0)\left(\frac{s}{s_0}\right)^\Delta, \tag{21}$$

$$R^2(s) = 4R_0^2 + 4\alpha'_{I\!P}ln(\frac{s}{s_0}), \tag{22}$$

and the soft profile is defined

$$\Gamma^S(s, b) = \frac{1}{\pi R^2(s)}\,e^{-\frac{b^2}{R^2(s)}}. \tag{23}$$

It is defined so as to keep the normalization $\int d^2b\,\Gamma^S(s, b) = 1$.

One has to distinguish between the eikonal model input and output. The key element is that the power Δ, and ν, are input information, not bounded by unitarity, and should not be confused with DL effective power ϵ and the corresponding total cross section. Since the DL model reproduces the forward elastic amplitude, in the ISR-HERA-Tevatron range, well, we require that the eikonal model output will be compatible with the DL results. Obviously, $\Delta > \epsilon$. In a non screened DL type model with a Gaussian profile the relation $B_{el} = \frac{1}{2}R^2(s)$ is exact. In a screened model, like GLM, $B_{el} > \frac{1}{2}R^2(s)$ due to screening.

With this input we get

$$\sigma_{tot} = 2\pi R^2(s)\left[ln\left(\frac{\nu(s)}{2}\right) + C - Ei\left(-\frac{\nu(s)}{2}\right)\right] \propto ln^2(s), \tag{24}$$

$$\sigma_{el} = \pi R^2(s)\left[ln\left(\frac{\nu(s)}{4}\right) + C - 2Ei\left(-\frac{\nu(s)}{2}\right) + Ei\left(-\nu(s)\right)\right] \propto \frac{1}{2}ln^2(s), \tag{25}$$

$$\sigma_{in} = \pi R^2(s)\{ln[\nu(s)] + C - Ei[-\nu(s)]\} \propto \frac{1}{2}ln^2(s). \tag{26}$$

$Ei(x) = \int_{-\infty}^{x}\frac{e^t}{t}dt$, and $C = 0.5773$ is the Euler constant. An important consequence of the above is that the ratio $\frac{\sigma_{el}}{\sigma_{tot}}$ is a single variable function of $\nu(s)$. In practice it means that given the experimental value of this ratio at a given energy we can obtain an "experimental" value of ν which does not depend on the adjustment of free parameters.

The formalism presented above is extended to diffractive channels through the observation, traced to Eqs.(3) and (14), that $P^S(s, b) = e^{-\Omega(s,b)}$. Accordingly, a screened non elastic diffractive cross section is obtained by convoluting its b-space amplitude square with the probability P^S.

The above has been utilized [30–33] to calculate the soft integrated single diffraction cross section. To this end, we write, in the triple Regge approximation [53], the double differential cross section $\frac{M^2 d\sigma_{sd}}{dM^2 dt}$, where M is the diffracted mass. We, then, transform it to b-space, multiply by $P^S(s, b)$ and integrate. The output $\frac{M^2 d\sigma_{sd}}{dM^2 dt}$, changes its high energy behaviour from $s^{2\Delta}$ modulu $ln(\frac{s}{s_0})$ (which is identical to the behaviour of a DL elastic cross section) to the moderate behaviour of $ln(\frac{s}{s_0})$. Note also a major difference in the diffractive b-space profile which changes from an input central Gaussian to an

output peripheral distribution peaking at higher b. Consequently, the GLM model is compatible with the Pumplin bound [54, 55].

$$\frac{\sigma_{el}(s,b) \, + \, \sigma_{diff}(s,b)}{\sigma_{tot}(s,b)} \, \leq \, \frac{1}{2}. \tag{27}$$

3.2 Extension to a multi channel model

The most serious deficiency of a single channel eikonal model is inherent, as the model considers only elastic rescatterings. This is incompatible with the relatively large diffractive cross section observed in the ISR-Tevatron energy range. To this we add a specific problematic feature of the GLM model. Whereas, σ_{tot}, σ_{el} and B_{el} are very well fitted, the reproduction of σ_{sd}, in the available ISR-Tevatron range, is poorer. A possible remedy to these deficiencies is to replace the one channel with a multi channel eikonal model, in which inelastic diffractive intermediate re-scatterings are included as well [38, 39, 56]. However, we have to insure that a multi channel model does improve the diffractive (specifically SD) predictions of the GLM model, while maintaining, simultaneously, its excellent reproductions [30–33] of the forward elastic amplitude, as well as its appealing results on LRG survival probabilities [35–37] to be discussed in **3.3**.

In the simplest approximation we consider diffraction as a single hadronic state. We have, thus, two orthogonal wave functions

$$\langle \Psi_h \mid \Psi_d \rangle \, = \, 0. \tag{28}$$

Ψ_h is the wave function of the incoming hadron, and Ψ_d is the wave function of the outgoing diffractive system initiated by the incoming hadron. Denote the interaction operator by **T** and consider two wave functions Ψ_1 and Ψ_2 which are diagonal with respect to **T**. The amplitude of the interaction is given by

$$A_{i,k} = \langle \Psi_i \Psi_k \mid \mathbf{T} \mid \Psi_{i'} \Psi_{k'} \rangle = a_{i,k} \, \delta_{i,i'} \, \delta_{k,k'}. \tag{29}$$

In a 2×2 model $i, k \, = \, 1, 2$. The amplitude $a_{i,k}$ satisfies the diagonal unitarity condition (see Eq.(13))

$$2Im \, a_{i,k}(s,b) \, = \mid a_{i,k}(s,b) \mid^2 \, + G_{i,k}^{in}(s,b), \tag{30}$$

for which we write the solution

$$a_{i,k}(s,b) \, = \, i \left(1 \, - \, e^{-\frac{\Omega_{i,k}(s,b)}{2}} \right), \tag{31}$$

and

$$G_{i,k}^{in} \, = \, 1 - e^{-\Omega_{i,k}(s,b)}. \tag{32}$$

$\Omega_{i,k}(s,b)$ is the opacity of the (i,k) channel with a wave function $\Psi_i \, \times \, \Psi_k$.

$$\Omega_{i,k} \, = \, \nu_{i,k}(s) \, \Gamma_{i,k}^{S}(s,b) \tag{33}$$

where

$$\nu_{i,k} \, = \, \sigma_{i,k}^{S0} \left(\frac{s}{s_0} \right)^{\Delta}. \tag{34}$$

The factorizable radii are given by

$$R_{i,k}^2(s) \, = \, 2R_{i,0}^2 \, + \, 2R_{0,k}^2 \, + \, 4\alpha'_{I\!\!P} ln(\frac{s}{s_0}). \tag{35}$$

$\Gamma_{i,k}^{S}(s,b)$ is the soft profile of the (i,k) channel. The probability that the final state of two interacting hadron states, with quantum numbers i and k, will be elastic regardless of the intermediate rescatterings is

$$P_{i,k}^{S}(s,b) \, = \, e^{-\Omega_{i,k}(s,b)} \, = \, \{1 \, - \, a_{i,k}(s,b)\}^2. \tag{36}$$

In the above diagonal representation, Ψ_h and Ψ_d can be written as

$$\Psi_h = \alpha\Psi_1 + \beta\Psi_2, \tag{37}$$

$$\Psi_d = -\beta\Psi_1 + \alpha\Psi_2. \tag{38}$$

Ψ_1 and Ψ_2 are orthogonal. Since $\mid \Psi_h \mid^2 = 1$, we have

$$\alpha^2 + \beta^2 = 1. \tag{39}$$

The wave function of the final state is

$$\begin{aligned}
\Psi_f = &\mid \mathbf{T} \mid \Psi_h \times \Psi_h\rangle = \\
&\alpha^2 a_{1,1}\{\Psi_1 \times \Psi_1\} + \alpha\beta a_{1,2}\{\Psi_1 \times \Psi_2 + \Psi_2 \times \Psi_1\} + \\
&\beta^2 a_{2,2}\{\Psi_2 \times \Psi_2\}.
\end{aligned} \tag{40}$$

We have to consider 4 possible re-scattering processes. However, in the case of a $\bar{p}p$ (or pp) collision, single diffraction at the proton vertex equals single diffraction at the antiproton vertex. i.e., $a_{1,2} = a_{2,1}$ and we end with three channels whose b-space amplitudes are given by

$$a_{el}(s,b) = \langle\Psi_h \times \Psi_h \mid \Psi_f\rangle = \alpha^4 a_{1,1} + 2\alpha^2\beta^2 a_{1,2} + \beta^4 a_{2,2}, \tag{41}$$

$$a_{sd}(s,b) = \langle\Psi_h \times \Psi_d \mid \Psi_f\rangle = \alpha\beta\{\alpha^2 a_{1,1} + (\alpha^2 - \beta^2)a_{1,2} + \beta^2 a_{2,2}\}, \tag{42}$$

$$a_{dd}(s,b) = \langle\Psi_d \times \Psi_d \mid \Psi_f\rangle = \alpha^2\beta^2\{a_{1,1} - 2a_{1,2} + a_{2,2}\}. \tag{43}$$

In the numeric calculations one may further neglect the double diffraction channel which is exceedingly small in the ISR-Tevatron range. This is obtained by setting $a_{2,2} = 2a_{1,2} - a_{1,1}$. Note that in the limit where $\beta << 1$, we reproduce the single channel model.

As in the single channel, we simplify the calculation assuming a Gaussian b-space distribution of the input opacities soft profiles

$$\Gamma_{i,k}^S(s,b) = \frac{1}{\pi R_{i,k}^2(s)} e^{-\frac{b^2}{R_{i,k}^2(s)}}. \tag{44}$$

The opacity expressions, just presented, allow us to express the physical observables of interest as functions of $\nu_{1,1}$, $\nu_{1,2}$, $R_{1,1}^2$, $R_{1,2}^2$ and β, which is a constant of the model. The determination of these variables enables us to produce a global fit to the total, elastic and diffractive cross sections as well as the elastic forward slope. This has been done in a two channel model, in which σ_{dd} is neglected [38]. The main conclusion of this study is that the extension of the GLM model to a multi channel eikonal results with a very good overall reproduction of the data. The results maintain the b-space peripherality of the diffractive output amplitudes and satisfy the Pumplin bound [54, 55]. Note that since different experimental groups have been using different algorithms to define diffraction, the SD experimental points are too scattered to enable a tight theoretical reproduction of the diffractive data, see Fig.2.

3.3   Survival probabilities of LRG in the GLM model

The eikonal model simplifies the calculation of the survival probability, Eq.(3), associated with the soft re-scatterings of the spectator partons. We can, thus, eliminate the nominator and denominator terms in $\mid M^H(s,b) \mid^2$ which depend exclusively on s. In the GLM model we assume a Gaussian b-dependence for $\mid M^H(s,b) \mid^2$ corresponding to a constant hard radius R^{H^2}. This choice enables an analytic solution of Eq.(3). More elaborate choices, such as dipole or multi poles distributions, require a numerical evaluation of this equation.
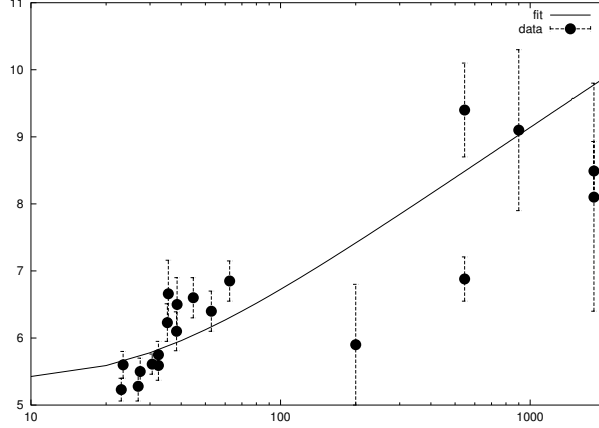
Fig. 2: Integrated SD data and a two channel model fit.

Define,

$$a_H(s) = \frac{R^2(s)}{R^{H\,2}(s)} > 1. \tag{45}$$

$a_H(s)$ grows logarithmically with s. As stated, Eq.(3) can be analytically evaluated with our choice of Gaussian profiles and we get

$$S^2 = \frac{a_H(s)\gamma[a_H(s), \nu(s)]}{[\nu(s)]^{a_H(s)}}, \tag{46}$$

where $\gamma(a, \nu)$ denotes the incomplete Euler gamma function

$$\gamma(a, x) = \int_0^x z^{a-1}e^{-z}dz. \tag{47}$$

The solution of Eq.(46), at a given s, depends on the input values of $R^{H\,2}$, R^2 and $\nu(s)$. In the GLM approach, $R^{H\,2}$ is estimated from the excellent HERA data [57–59] on $\gamma + p \rightarrow J/\Psi + p$. The values of $\nu(s)$ and $R^2(s)$ are obtained from the experimental $\bar{p}p$ data. This can be attained from a global fit to the soft scattering data [38]. Alternatively, we can obtain ν from the ratio $\frac{\sigma_{el}}{\sigma_{tot}}$ and then obtain the value of R^2 from the explicit expressions given in Eqs.(24,25,26). LHC predictions presently depend on model calculations with which this information can be obtained. Once we have determined $\nu(s)$ and $a_H(s)$, the survival probability is calculated from Eq.(46).

In the GLM three channel model we obtain for central hard diffraction of di-jets or Higgs a survival probability,

$$S_{CD}^2(s) = \frac{\int d^2b \left(\alpha^4\, P_{1,1}^S\, \Omega_{1,1}^{H\,2} + 2\alpha^2\beta^2\, P_{1,2}^S\, \Omega_{1,2}^{H\,2} + \beta^4 P_{2,2}^S\, \Omega_{2,2}^{H\,2}\right)}{\int d^2b \left(\alpha^4\, \Omega_{1,1}^{H\,2} + 2\alpha^2\beta^2\, \Omega_{1,2}^{H\,2} + \beta^4\, \Omega_{2,2}^{H\,2}\right)}. \tag{48}$$

The hard diffractive cross sections in the (i,k) channel are calculated using the multi particle optical theorem [53]. They are written in the same form as the soft amplitudes

$$\Omega_{i,k}^{H\,2} = \nu_{i,k}^{H}(s)^2\, \Gamma_{i,k}^{H}(b), \tag{49}$$

where,

$$\nu_{i,k}^{H} = \sigma_{i,k}^{H0}\left(\frac{s}{s_0}\right)^{\Delta_H}. \tag{50}$$

As in the single channel calculation we assume that $\Gamma_{i,k}^H(b)$ is Gaussian,

$$\Gamma_{i,k}^H(b) = \frac{2}{\pi R_{i,k}^2} e^{-\frac{2\,b^2}{R_{i,k}^2}}.$$ (51)

Note, that the hard radii $R_{i,k}^{H\,2}$ are constants derived from HERA J/Ψ photo and DIS production [57–59].

As it stands, a three channel calculation is not useful since σ_{dd} is very small and the 3'd channel introduces additional parameters which can not be constraint by the meager experimental information on σ_{dd} [13–17]. In a two channel model Eq.(48) reduces to

$$S_{CD}^2(s) = \frac{\int d^2b \left(P_{1,1}^S \, \Omega_{1,1}^{H\,2} - 2\beta^2 \left(P_{1,1}^S \, \Omega_{1,1}^{H\,2} - P_{1,2}^S \, \Omega_{1,2}^{H\,2} \right) \right)}{\int d^2b \left(\Omega_{1,1}^{H\,2} - 2\beta^2 \left(\Omega_{1,1}^{H\,2} - \Omega_{1,2}^{H\,2} \right) \right)}.$$ (52)

A new, unpublished yet, model [60], offers an explicit S^2 calculation for the exclusive $NN \rightarrow N + LRG + 2J + LRG + N$ final state, both in one and two channel eikonal models. We shall comment on its output in the next subsection.

3.4   GLM S^2 predictions

Following are a few general comments on the GLM calculations of S^2, after which we discuss the input/output features of the single and two channel models. Our objective is to present predictions for LHC.

The only available experimental observable with which we can check the theoretical S^2 predictions is the hard LRG di-jets data obtained in the Tevatron and Hera. A comparison between data and our predictions is not immediate as the basic measured observable is f_{gap} and not S^2. The application of the GLM models to a calculation of f_{gap} depends on an external input of a hard diffractive LRG cross section which is then corrected by S^2 as presented above. Regardless of this deficiency, the introduction of a survival probability is essential so as to understand the huge difference between the pQCD calculated F_{gap} and its experimental value f_{gap}. A direct test of the GLM predictions calls for a dedicated experimental determination of S^2. The only direct S^2 information from the Tevatron is provided by a JGJ ratio measured by D0 [5–7] in which $\frac{S^2(\sqrt{s}=630)}{S^2(\sqrt{s}=1800)} = 2.2 \pm 0.8$. This is to be compared with a GLM ratio of $1.2 - 1.3 \pm 0.4$ presented below.

The survival probabilities of the CD, SD and DD channels are not identical. The key difference is that each of the above channels has a different hard radius. A measure of the sensitivity of S^2 to changes in ν and a_H is easy to identify in a single channel calculation which is presented in Fig.3. Indeed, preliminary CDF GJJG data [17] suggest that f_{gap} measured for this channel is moderately smaller than the rate measured for the GJJ channel.

GLM soft profile input is a central Gaussian. This is over simplified, and most models assume a power like dipole or multipole b-dependence of $\Gamma^S(s,b)$ and $\Gamma^H(s,b)$. Explicit comparisons [60] of S^2 obtained with different input profiles shows a diminishing difference between the survival probability outputs, provided their effective radii are compatible.

Regardless of the attractive simplicity of the single channel model, one should add a cautious reminder that the single channel model does not reproduce σ_{sd} well since its survival probabilities are over-estimated. Consequently, we are inclined to suspect that the S^2 values presented in Table 1 are over-estimated as well.

As we noted, the soft input can be obtained from either a model fit to the soft scattering data or directly from the measured values of $\sigma_{tot}, \sigma_{el}$ and $R^{H\,2}$. The first method is denoted F1C and the second is denoted D1C. Note that having no LHC data, $S_{DD}^2(D1C)$, at this energy, is calculated on the
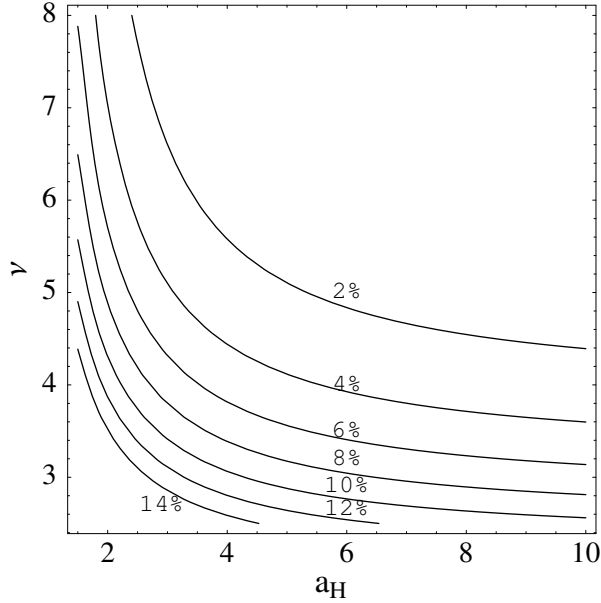
Fig. 3: A contour plot of $S^2(1C)$ against $\nu(s)$ and $a_H(s)$.

Table 1: Survival probabilities

$\sqrt{s}$ (GeV)	$S^2_{\text{CD}}(\text{F1C})$	$S^2_{\text{CD}}(\text{D1C})$	$S^2_{\text{SD}_{\text{incl}}}(\text{F1C})$	$S^2_{\text{SD}_{\text{incl}}}(\text{D1C})$	$S^2_{\text{DD}}(\text{F1C})$	$S^2_{\text{DD}}(\text{D1C})$
540	14.4%	13.1%	18.5%	17.5%	22.6%	22.0%
1800	10.9%	8.9%	14.5%	12.6%	18.2%	16.6%
14000	6.0%	5.2%	8.6%	8.1%	11.5%	11.2 %

basis of model estimates for the total and elastic cross sections. The constant hard radius $R^{H^2} = 7.2$ is deduced from HERA J/Ψ photoproduction forward exponential slope which shows only diminishing shrinkage [57,58]. This is a conservative choice which may be changed slightly with the improvement of the Tevatron CDF estimates [61] of R^{H^2}. The two sets of results obtained are compatible, even though, $S^2(D1C)$ is consistently lower than $S^2(F1C)$. The S^2 output presented above depends crucially on the quality of the data base from which we obtain the input parameters. The two sets of Tevatron data at $1800\,GeV$ have a severe $10-15\%$ difference resulting in a non trivial ambiguity of the S^2 output.

The global GLM two channel fit [38] reproduces the soft scattering data (including SD) remarkably well with $\beta = 0.464$. Its fitted parameters are used for the soft input required for the S^2 calculations. Our cross section predictions for LHC are: $\sigma_{tot} = 103.8\,mb$, $\sigma_{el} = 24.5\,mb$, $\sigma_{sd} = 12\,mb$ and $B_{el} = 20.5\,GeV^{-2}$. The input for the calculation of S^2 requires, in addition to the soft parameters, also the values of $\nu^H_{i,k}$ and $R^H_{i,k}{}^2$. The needed hard radii can be estimated, at present, only for the CD channel, where we associate the hard radii $R^H_{1,1}$ with the hard radius obtained in HERA exclusive J/Ψ photoproduction [57,58] and $R^H_{1,2}$ with HERA inclusive J/Ψ DIS production [59]. Accordingly, we have $R^H_{1,1}{}^2 = 7.2\,GeV^{-2}$, and $R^H_{1,2}{}^2 = 2.0\,GeV^{-2}$. We do not have experimental input to determine $\nu^H_{i,k}$. We overcome this difficalty by assuming a Regge-like factorization $\sigma^{H0}_{i,k}/\sigma^{S0}_{i,k} = constant$. Our predictions for the CD survival probabilities are: 6.6% at $540\,GeV$, 5.5% at $1800\,GeV$ and 3.6% at $14000\,GeV$.

These results may be compared with a recent, more elaborate, eikonal formulation [60] aiming to calculate the survival probability of a final exclusive $N + LRG + 2J(orH) + LRG + N$ state. These calculations were done in one and two channel models. The one channel S^2_{CD} predicted values are 14.9%

at $540\,GeV$, 10.8% at $1800\,GeV$ and 6.0% at $14000\,GeV$. These values are remarkably similar to the GLM one channel output. In the two channel calculations the corresponding predictions are 5.1%, 4.4% and 2.7%, which are marginally smaller than the GLM two channel output numbers.

In our assessment, the two channel calculations provide a more reliable estimate of S^2 since they reproduce well the soft scattering forward data. Our estimate for the survival probability associated with LHC Higgs production is $2.5\% - 4.0\%$.

4   The KKMR Model

The main part of this section (**4.1-4.3**) was written by V.A. Khoze, A.D. Martin and M. Ryskin (KMR) and is presented here without any editing.

The KKMR model calculation [40–44] of the survival probabilities is conceptually quite similar to the GLM model, in as much as unitarization is enforced through an eikonal model whose parameters provide a good reproduction of the high energy soft scattering data. However, the GLM model is confined to a geometrical calculation of S^2 for which we need just the value of R^{H2}, without any specification of the hard dynamics. This value is an external input to the model. The KKMR model contains also a detailed pQCD calculation of the hard diffractive proccess, specifically, central diffractive Higgs production. Consequently, it can predict a cross section for the channel under investigation.

4.1   KKMR model for soft diffraction

The KMR description [41] of soft diffraction in high energy pp (or $p\bar{p}$) collisions embodies

 (i) *pion-loop* insertions in the bare Pomeron pole, which represent the nearest singularity generated by t-channel unitarity,

 (ii) a *two-channel eikonal* which incorporates the Pomeron cuts generated by elastic and quasi-elastic (with N^* intermediate states) s-channel unitarity,

(iii) high-mass *diffractive dissociation*.

The KKMR model gives a good description of the data on the total and differential elastic cross section throughout the ISR-Tevatron energy interval, see [41]. Surprisingly, KMR found the bare Pomeron parameters to be

$$\Delta \equiv \alpha(0) - 1 \simeq 0.10, \qquad \alpha' = 0. \tag{53}$$

On the other hand it is known that the same data can be described by a simple effective Pomeron pole with [47, 48, 62]

$$\alpha_{I\!P}^{\text{eff}}(t) = 1.08 + 0.25\,t. \tag{54}$$

In this approach the shrinkage of the diffraction cone comes not from the bare pole ($\alpha' = 0$), but has components from the three ingredients, (i)–(iii), of the model. That is, in the ISR-Tevatron energy range

$$``\alpha'_{\text{eff}}" = (0.034 + 0.15 + 0.066)\,\text{GeV}^{-2} \tag{55}$$

from the π-loop, s-channel eikonalisation and diffractive dissociation respectively. Moreover, eikonal rescattering suppresses the growth of the cross section and so $\Delta \simeq 0.10 > \Delta_{\text{eff}} \simeq 0.08$.

Since the model [41] embodies all the main features of soft diffraction KMR expect it to give reliable predictions for the *survival probability* S^2 of the rapidity gaps against population by secondary hadrons from the underlying event, that is hadrons originating from soft rescattering. In particular, KMR predict $S^2 = 0.10\ (0.06)$ for single diffractive events and $S^2 = 0.05\ (0.03)$ for exclusive Higgs boson production, $pp \to p + H + p$, at Tevatron (LHC) energies.
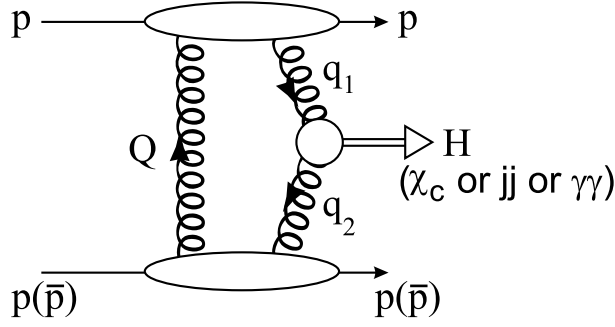
Fig. 4: Schematic diagram for central exclusive production, $pp \rightarrow p + X + p$. The presence of Sudakov form factors ensures the infrared stability of the Q_t integral over the gluon loop. It is also necessary to compute the probability, S^2, that the rapidity gaps survive soft rescattering.

4.2 Calculation of the exclusive Higgs signal

The basic mechanism for the exclusive process, $pp \rightarrow p + H + p$, is shown in Fig. 4. The left-hand gluon Q is needed to screen the colour flow caused by the active gluons q_1 and q_2. Since the dominant contribution comes from the region $\Lambda_{\rm QCD}^2 \ll Q_t^2 \ll M_H^2$, the amplitude may be calculated using perturbative QCD techniques [40,63]

$$\mathcal{M}_H \simeq N \int \frac{dQ_t^2}{Q_t^4} f_g(x_1, x_1', Q_t^2, \mu^2) f_g(x_2, x_2', Q_t^2, \mu^2), \tag{56}$$

where the overall normalisation constant N can be written in terms of the $H \rightarrow gg$ decay width [40,64]. The probability amplitudes (f_g) to find the appropriate pairs of t-channel gluons (Q, q_1) and (Q, q_2) are given by the skewed unintegrated gluon densities at the hard scale μ, taken to be $0.62\, M_H$. Since the momentum fraction x' transfered through the screening gluon Q is much smaller than that (x) transfered through the active gluons $(x' \sim Q_t/\sqrt{s} \ll x \sim M_H/\sqrt{s} \ll 1)$, it is possible to express $f_g(x, x', Q_t^2, \mu^2)$, to single log accuracy, in terms of the conventional integrated density $g(x)$ [65–68]. The f_g's embody a Sudakov suppression factor T, which ensures that the gluon does not radiate in the evolution from Q_t up to the hard scale $\mu \sim M_H/2$, and so preserves the rapidity gaps.

It is often convenient to use the simplified form [40]

$$f_g(x, x', Q_t^2, \mu^2) = R_g \frac{\partial}{\partial \ln Q_t^2} \left[\sqrt{T_g(Q_t, \mu)}\, xg(x, Q_t^2) \right], \tag{57}$$

which holds to 10–20% accuracy.[1] The factor R_g accounts for the single $\log Q^2$ skewed effect [67]. It is found to be about 1.4 at the Tevatron energy and about 1.2 at the energy of the LHC.

4.3 The Sudakov factor

The Sudakov factor $T_g(Q_t, \mu)$ reads [65,66,69]

$$T_g(Q_t, \mu) = \exp\left(-\int_{Q_t^2}^{\mu^2} \frac{\alpha_S(k_t^2)}{2\pi} \frac{dk_t^2}{k_t^2} \left[\int_\Delta^{1-\Delta} z P_{gg}(z) dz + \int_0^1 \sum_q P_{qg}(z) dz \right] \right), \tag{58}$$

with $\Delta = k_t/(\mu + k_t)$. The square root arises in (57) because the (survival) probability not to emit any additional gluons is only relevant to the hard (active) gluon. It is the presence of this Sudakov factor which makes the integration in (56) infrared stable, and perturbative QCD applicable[2].

---

[1]In the actual computations a more precise form, as given by Eq. (26) of [68], was used.

[2]Note also that the Sudakov factor inside t integration induces an additional strong decrease (roughly as M^{-3} [44]) of the cross section as the mass M of the centrally produced hard system increases. Therefore, the price to pay for neglecting this suppression effect would be to considerably overestimate the central exclusive cross section at large masses.

Table 2: Compilation of S^2 values obtained in the KKMR model

$\sqrt{s}$ (GeV)	$S^2_{2C}(CD)$	$S^2_{2C}(SD_{incl})$	$S^2_{2C}(DD)$
540	6.0%	13.0%	20.0%
1800	4.5%	10.0%	15.0%
14000	2.6%	6.0%	10.0%

It should be emphasized that the presence of the double logarithmic T-factors is a purely classical effect, which was first discussed in 1956 by Sudakov in QED. There is strong bremsstrahlung when two colour charged gluons 'annihilate' into a heavy neutral object and the probability not to observe such a bremsstrahlung is given by the Sudakov form factor[3]. Therefore, any model (with perturbative or non-perturbative gluons) must account for the Sudakov suppression when producing exclusively a heavy neutral boson via the fusion of two coloured particles.

More details of the role of the Sudakov suppression can be found in J. Forshaw's review in these proceedings [34]. Here KMR would like to recall that the T-factors in [44, 70] were calculated to *single* log accuracy. The collinear single logarithms were summed up using the DGLAP equation. To account for the 'soft' logarithms (corresponding to the emission of low energy gluons) the one-loop virtual correction to the $gg \to H$ vertex was calculated explicitly, and then the scale $\mu = 0.62\,M_H$ was chosen in such a way that eq.(58) reproduces the result of this explicit calculation. It is sufficient to calculate just the one-loop correction since it is known that the effect of 'soft' gluon emission exponentiates. Thus (58) gives the T-factor to single log accuracy.

In some sense, the T-factor may be considered as a 'survival' probability not to produce any hard gluons during the $gg \to H$ fusion subprocess. However, it is not just a number (i.e. a numerical factor) which may be placed in front of the integral (the 'bare amplitude'). Without the T-factors hidden in the unintegrated gluon densities f_g the integral (56) diverges. From the formal point of view, the suppression of the amplitude provided by T-factors is infinitely strong, and without them the integral depends crucially on an ad hoc infrared cutoff.

4.4 Summary of KKMR S^2 predictions

Table 2 shows a compilation of S^2 values in the KKMR model. A comparison with the corresponding GLM two channel model is possible only for the available GLM CD channel, where, the KKMR output is compatible with GLM. KKMR SD and DD output are compatible with the corresponding GLM single channel numbers. Overall, we consider the two models to be in a reasonable agreement.

A remarkable utilization of the KKMR model is attained when comparing the HERA [18–27] and CDF [8–12, 17] di-jets diffractive structure functions derived for the dynamically similar GJJ channels. To this end, the comparison is made between the kinematically compatible HERA $F^D_{jj}(Q^2 = 75\,GeV^2, \beta)$ and the CDF $F^D_{jj}(<E^2_T> = 75\,GeV^2, \beta)$. The theoretical expectation is that $F^D_{jj}(\beta)$, as measured by the two experiments, should be very similar. As can be seen in Fig.5, the normalizations of the two distributions differ by approximately an order of magnitude and for very small $\beta < 0.15$ there is a suggestive change in the CDF distribution shape. This large discrepancy implies a breaking of QCD and/or Regge factorization. Reconsidering, it is noted, that HERA DIS data is measured at a high Q^2 where the partonic interactions induced by the highly virtual photon are point like and, hence, $S^2 = 1$. On the other hand, CDF GJJ measurement is carried out at $1800\,GeV$ and, as we saw, its survival prob-

---

[3]It is worth mentioning that the $H \to gg$ width and the normalization factor N in (56) is an 'inclusive' quantity which includes all possible bremsstrahlung processes. To be precise, it is the sum of the $H \to gg + ng$ widths, with n=0,1,2,... . The probability of a 'purely exclusive' decay into two gluons is nullified by the same Sudakov suppression.
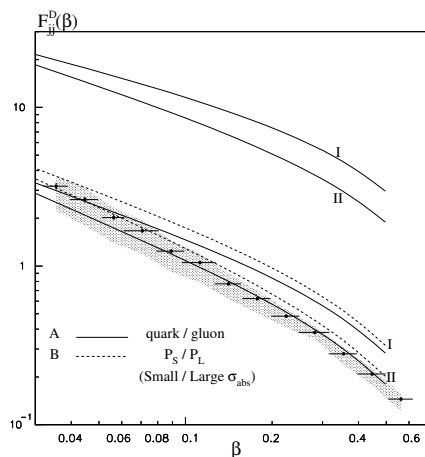
Fig. 5: The predictions for the diffractive di-jets production at the Tevatron (lower lines), obtained from two alternative sets of HERA diffractive parton distributions I and II, compared with the CDF data (shaded area). The upper lines correspond to the Tevatron prediction neglecting the survival probability correction.

ability is rather small. The convolution between the HERA determined GJJ $F_{jj}^D(\beta)$ and the β dependent survival probabilities, as calculated by KKMR, provides the $F_{jj}^D(\beta)$ distribution corrected for the soft rescattering of the spectator partons. This is shown in Fig.5 and provides an impressive reproduction of the experimental distribution. We were informed [71] that this analysis was successfully redone with an updated H1 produced structure function distribution.

The weak element in the above analysis is that it is crucially dependent on the H1 determined $F_{jj}^D(\beta)$ distribution. ZEUS has constructed a somewhat different structure function. Clearly, a very different experimental determination of $F_{jj}^D(\beta)$, such as been recently suggested by Arneodo [72], will re-open this analysis for further studies, experimental and theoretical.

4.5 A Comparison between KKMR and GLM

The approach of GLM and KKMR to the calculation of forward soft scattering in the ISR-Tevatron range are basically similar. Both models utilize the eikonal model assuming different input soft profiles which have, nevertheless, compatible effective radii. There are, though, a few particular differences between the two sets of calculations:

1) The GLM model, with a Gaussian soft profile, is applicable only in the forward cone ($|t| < 0.3\,GeV^2$), where we have most of the data of interest. KKMR use a multipole power behaviour profile which enables applicability over a, somewhat, wider t range, $|t| < 0.5\,GeV^2$. Note that, the GLM output is not significantly changed with a multipole power behaviour profile provided its radii are compatible with the Gaussian input [60].

2) The GLM input Pomeron trajectory is specified by $\Delta = 0.12$ and $\alpha'_{I\!P} = 0.2$. These evolve due to eikonalisation to an effective output of $\epsilon = 0.08$ and $\alpha'_{I\!P} = 0.25$. Note that, Δ is obtained in GLM as a fitted output parameter. In KKMR, the relatively high input $\Delta \simeq 0.2$ is theoretically tuned by a pion loop renormalization resulting in an input value of $\Delta \simeq 0.1$. KKMR have a more elaborate treatment of $\alpha_{I\!P}(t)$ than GLM, resulting, nevertheless, with forward cone output predictions similar to GLM. However, KKMR accounts for a somewhat wider t range than GLM and reproduces the t dependence of B_{el} well. Similar results are obtained in a GLM version [39,56] in which the soft profile is given by a dipole distribution. KKMR can predict a few differential properties of S^2, which are beyond the scope of GLM.

3) Both models treat the high mass diffraction with the triple Pomeron formalism [53]. In GLM the final SD cross section is obtained by a convolution of the input $\frac{d\sigma_{sd}}{d^2b}$ with $P^S(s,b)$. In KKMR the treatment of the SD amplitude is more elaborate, ending, though, with no detailed SD data reconstruction which is presented in GLM.

4) The LHC predictions of the two models for cross sections and slopes are compatible, with the exception of σ_{dd} which is neglected in GLM and acquires a significant KKMR predicted value of $9.5\,mb$.

GLM is a geometrical model where both the input hard LRG non corrected matrix element squared and the soft elastic scattering amplitude, are approximated by central Gaussians in b-space. This property enables us to easily calculate the survival probabilities which depend on ν, R^2 and $R^{H\,2}$ in a single channel input, and on $\nu_{i,k}$, $R^2_{i,k}$ and $R^{H\,2}_{i,k}$ in a two channel input. As we have noted, the GLM model, on its own, cannot provide a calculation of F_{gap} and f_{gap} as it needs the hard radii as an external input. The KKMR model is more sophisticated. This is attributed to the fact that the hard diffractive LRG process is explicitly calculated in pQCD, hence the non corrected F_{gap} and the corrected f_{gap} and F^D_{jj} are model predictions. As we have just noted, given the hard diffractive matrix element, the actual calculation of the diffractive LRG survival probability damping is almost identical to GLM. Keeping this basic observation in mind, it is constructive to compare the features of the two models with a special interest on the input assumptions and output differences of the two models.

The main difference between the two models is reflected in the level of complexity of their inputs. GLM soft input is obtained from a simple eikonal model for the soft forward scattering, to which we add the hard radii which are derived from the HERA data. KKMR calculations of P^S are equally simple. The calculation of the hard sector matrix elements are, naturally, more cumbersome. Given HERA $F^D_{jj}(Q^2, \beta)$, a Tevatron diffractive F^D_{jj} in which $< E_T >$ and Q^2 are comparable, can be calculated, parameter free, without the need to calculate the hard amplitude. But this is a particular case and, in general, the KKMR calculation depends on an extended parameter base, such as the the input p.d.f. and pQCD cuts. These input parameters are not constrained tightly enough.

The elaborate structure of the KKMR model provides a rich discovery potential which is reflected in the model being able to define and calculate the dependence of S^2 not only on b, but also on other variables, notably β, and experimental cuts such as the recoil proton transverse momentum. GLM depends on the hard radii external information obtained from HERA data. It lacks the potential richness of KKMR. GLM can serve, though, as a standard through which we can compare different unitarized models. Given such a model, we can extract effective values for ν, R^2 and $R^{H\,2}$ and proceed to a simple calculation of S^2. We shall return to this proposed procedure in the final discussion.

Even though both GLM and KKMR are two channel models, they are dynamically different. GLM two channel formulation relates to the diversity of the intermediate soft re-scatterings, i.e. elastic and diffractive for which we have different soft amplitudes $a_{i,k}$, each of which is convoluted with a different probability $P^S_{i,k}$ which depends on a different interaction radius $R^2_{i,k}$. In the KKMR model the two channels relate to two different dynamical options of the hard process. In model A the separation is between valence and sea interacting partons. In model B the separation is between small and large dipoles. The two models give compatible results. The key point, though, is that the KKMR opacities $\Omega_{i,k}$, in the definition of $P^S_{i,k}$, differ in their normalization, but have the same b-dependence. Regardless of this difference the output of the GLM and KKMR models is reasonably compatible. The compatibility between GLM and KKMR is not surprising since the explicit KKMR calculation of the hard LRG amplitude is approximated relatively well by the GLM simple Gaussian.

Our final conclusion is that the two model output sets are compatible. The richness of the KKMR model has a significant discovery potential lacking in GLM. On the other hand, the GLM simplicity makes it very suitable as a platform to present different models in a uniform way, which enables a transparent comparison.

5 Discussion

As we shall see, at the end of this section, there is no significant difference between the values of σ_{tot} predicted by DL and GLM up to the top Cosmic Rays energies. This is, even though, DL is a Regge model without unitarity corrections. The explanation for this "paradox" is that the DL amplitude violations of s-unitarity are confined, even at super high energies, to small b which does not contribute significantly to σ_{tot}. Note, though, that $\frac{\sigma_{el}}{\sigma_{tot}}$ grows in DL like s^ϵ whereas in GLM its growth is continuosly being moderated with increasing s (see table in **5.3**). The DL model predicts that S^2 is identical to unity or very close to it in the DL high-t model where a weak $I\!P I\!P$ cut is added. The need for survival probabilities so as to reproduce the the experimental soft SD cross section values and the hard di-jets rates, is the most compelling evidence in support of unitarization at presently available energies. As such, the study of high energy soft and hard diffraction serves as a unique probe substantiating the importance of s-channel unitarity in the analysis of high energy scattering.

5.1 S^2 in unitarized models

Most, but not all, of the unitarized models dealing with LHC S^2 predictions have roughly the same S^2 values. This calls for some clarifications. The first part of our discussion centers on the correlated investigation of two problems:

1) How uniform are the output predictions of different unitarization procedures?
2) How sensitive are the eikonal calculations to the details of the eikonal model they use?

We start with two non eikonal models which have contradictory predictions.

The first is a model suggested by Troshin and Tyurin [52]. In this model the single channel unitarity constraint (Eq.(13)) is enforced with an asymptotic bound where $G_{in} = 0$ and $|a_{el}| = 2$ i.e. asymptotically, $\sigma_{tot} = \sigma_{el}$ and $P^S(s,b) = 1$. The parameters of the model are set so as to obtain a "normal" survival probability monotonically decreasing with energy up to about $2500\,GeV$ where it changes its behavior and rises monotonically to its asymptotic limit of 1. Beside the fact that the model has a legitimate but non appealing asymptotics, its main deficiency is that it suggests a dramatic change in the systematics of S^2 without being able to offer any experimental signature to support this claim. Regardless of this criticism, this is a good example of a proper unitarity model whose results are profoundly different from the eikonal model predictions.

Another non eikonal procedure is Goulianos flux renormalization model [17]. This is a phenomenological model which formally does not enforce unitarity, but rather, a bound of unity on the Pomeron flux in diffractive processes. Note that, the Pomeron flux is not uniquely defined so this should be regarded as an ad hoc parametrization. Nevertheless, it has scored an impressive success in reproducing the soft and hard diffractive data in the ISR-Tevatron range. The implied survival probabilities of this procedure are compatible with GLM and KKMR. However, the model predicts suppression factors for the diffractive channels which are t-independent and, thus, b-independent. The result is that, even though the output diffractive cross section is properly reduced relative to its input, there is no change of the output profile from its input Gaussian form. Consequently, the Pumplin bound is violated. We are informed that Goulianos plans to improve his model by eikonalizing the output of his present model.

As noted, there are a few eikonal models on the market [73–80], and their predictions are compatible with GLM and KKMR. Reconsidering the procedure of these calculations, their compatibility is not surprising once we translate their input to a GLM format. The GLM eikonal S^2 calculation has two input sectors in either a single or a two channel version. They are the soft ν and R^2, and the hard radius R^{H^2}. Since the soft input is based on a fit of the soft scattering data base, the potential variance in the soft parameters is relatively small. The input hard radius is obtained from either the HERA data or a theoretical calculation, be it a pQCD diagram or a Regge model. All in all, this is a reasonably stable input. In this context, it is interesting to discuss the eikonal model of Block and Halzen [73], where

the calculated survival probabilities for Higgs production through W-W fusion are seemingly too high, $S^2(540) = 27\%$, $S^2(1800) = 21\%$ and $S^2(14000) = 13\%$. Even though, Higgs production is a CD process, the above S^2 values are in agreement with the KKMR calculations of S^2_{DD} with a relatively high $R^{H^2} = 11\,GeV^{-2}$. In a proper S^2_{CD} calculation, these high S^2 values correspond to an even higher $R^{H^2} \simeq 20\,GeV^{-2}$, which is far too high as an estimate of the hard radius of $WW \to H$. A possible interpretation of Block-Halzen results is to associate them with a soft, rather than a hard, LRG CD process. This would couple with the non screened interpretation of CD Higgs through the soft CEM model [74, 75], which predicts very high S^2 values. Since the CEM model is not screened we may, as well, assign a survival probability to its output result. This translates into $S^2_{CD} = S^2_{BH} S^2_{CEM}$, providing rather reasonable one channel predictions, $S^2_{CD}(540) = 18.9\%$ and $S^2_{CD}(1800) = 7.2\%$.

Obviously, each of the eikonal models, quoted above has its own particular presentation and emphasis. They do, however, have compatible results reflecting the observation that their input translates into similar values of ν, R^2 and R^{H^2}.

5.2 Compatibility between HERA and the Tevatron di-jets data

Much attention has been given recently to the compatibility between the Tevatron and HERA DIS GJJ data. The starting point made by KKMR and CDF is that rather than depend on a p.d.f. input to calculate F_{gap}, we may use, the GJJ di-jets diffractive structure function, F^D_{jj}, inferred from HERA DIS data [18–27] and associate it with the F^D_{jj} derived from the Tevatron GJJ data. As it stands, this procedure ignores the role of the survival probability. Consequently, F^D_{jj} obtained from the Tevatron is an order of magnitude smaller than the HERA output [8–12, 17, 40–44]. This result led to speculations about a possible breaking of QCD or Regge factorization or both. Once the Tevatron di-jets diffractive structure function is rescaled by the appropriate survival probability, the compatibility between the Tevatron and HERA DIS diffractive data is attained. The conclusion of this analysis is that the breaking of factorization is attributed to the soft re-scatterings of the the colliding projectiles. Additional hard contribution to the factorization breaking due to gluon radiation is suppressed by the Sudakov factor included in the pQCD calculation (see **4.3**).

One should note, though, that the H1 determination [18–27] of F^D_{jj} is not unique. Arneodo [72] has suggested a different F^D_{jj} output based on HERA di-jets data which has a different normalization and β dependences. Should this be verified, there might well be a need to revise the KKMR calculations.

The evolution of HERA F^D_{jj} from high Q^2 DIS to $Q^2 = 0$ di-jets photoproduction has raised additional concern with regard to the validity of the factorization theorems [28, 29]. This is a complicated analysis since one has to be careful on two critical elements of the calculations:

1) The determination of the ratio between direct and resolved exchanged photon (real or virtual). This is a crucial element of the theoretical calculation since survival probability is applicable only to the resolved photon component. For very high Q^2 data the hard scattering process with the target partons is direct. At $Q^2 = 0$ there is a significant resolved photon contribution.

2) For di-jets production there is a big difference between the LO and the NLO pQCD calculated cross sections [81–83]. Since the HERA analysis compares the pQCD calculation with the di-jets measured cross section the normalization and shape of the theoretical input is most crucial in the experimental comparison between the high Q^2 and $Q^2 = 0$ data.

On the basis of a NLO calculation, Klasen and Kramer [81, 82] conclude that they can reproduce the photoproduction data with $S^2 = 0.34$, applied to the resolved sector. This survival probability is in agreement with KKMR and GLM calculations.

Regardless of the above, preliminary photoproduction GJJ HERA data [28, 29] suggest that both the direct and resolved photon sectors are suppressed at $Q^2 = 0$. A verification of this observation has

Table 3: GLM two-channel predictions at a few energies

$\sqrt{s}$ [GeV]	$\sigma_{\text{tot}}^{\text{DL}}$ [mb]	$\sigma_{\text{tot}}^{\text{GLM}}$ [mb]	$\sigma_{\text{el}}^{\text{GLM}}$ [mb]	$\sigma_{\text{sd}}^{\text{GLM}}$ [mb]	$B_{\text{el}}^{\text{GLM}}$ [GeV^{-2}]	$S_{\text{CD}}^{\text{GLM}\,2}$
540	60.1	62.0	12.3	8.7	14.9	0.066
1800	72.9	74.9	15.9	10.0	16.8	0.055
14000	101.5	103.8	24.5	12.0	20.5	0.036
30000	114.8	116.3	28.6	12.7	22.0	0.029
60000	128.4	128.7	32.8	13.2	23.4	0.023
90000	137.2	136.5	35.6	13.5	24.3	0.019
120000	143.6	142.2	37.6	13.7	24.9	0.017

severe consequences for our understanding of the evolution of the diffractive structure function from DIS to photoproduction. It does not directly relate, though, to the issue of soft survival probability which apply, per definition, only to the resolved photon sector. The suggested effect in the direct photon sector should, obviously be subject to a good measure of caution before being substantiated by further independent analysis.

5.3 Diffraction at energies above the LHC

We end with Table 3, which shows the GLM two channel predictions for energies including the LHC, and up to the top Cosmic Rays energies. The, somewhat, surprizing observation is that the GLM calculated total cross sections are compatible with the DL simple Regge predictions all over the above energy range. This is a reflection of the fact that even at exceedingly high energies unitarization reduces the elastic amplitude at small enough b values to be relatively insensitive to the calculation of σ_{tot}. On the other hand, we see that σ_{el} becomes more moderate in its energy dependence and σ_{el}/σ_{tot} which is 23.6% at the LHC is no more than 26.4% at the highest Cosmic Rays energy, $120\,TeV$. The implication of this observation is that the nucleon profile becomes darker at a very slow rate and is grey (well below the black disc bound) even at the highest energy at which we can hope for a measurment. A check of our results at the Planck scale shows $\sigma_{tot} = 1010\,mb$ and the profile to be entirely black. i.e., $\frac{\sigma_{el}}{\sigma_{tot}} = \frac{1}{2}$. σ_{sd} is even more moderate in its very slow rise with energy. The diminishing rates for soft and hard diffraction at exceedingly high energies are a consequence of the monotonic reduction in the values of S^2 with a Planck scale limit of $S^2 = 0$. This picture is bound to have its effect on Cosmic Rays studies.

Our LHC predictions are compatible with KMR. Note, though, that: i) σ_{sd}^{GLM} is rising slowly with s gaining 20% from the Tevatron to LHC. KMR has a much faster rise with energy, where, σ_{sd}^{KMR} is gaining $77\% - 92\%$ over the same energy interval. ii) At the LHC $B_{el}^{GLM} = 20.5\,GeV^{-2}$, to be compared with a DL slope of $19\,GeV^{-2}$ and a KMR slope of $22\,GeV^{-2}$. The GLM $30\,TeV$ cross sections are compatible with Block-Halzen.

6 Acknowledgements

Appendix: Monte Carlo modeling of gap survival

The following was contributed by Leif Lönnblad and is presented without any editing.

An alternative approach to gap survival and factorization breaking is to implement multiple interactions in Monte Carlo event generators. These models are typically based on the eikonalization of the partonic cross section in hadronic collisions and can be combined with any hard sub process to describe the additional production of hadrons due to secondary partonic scatterings. Some of these programs, such as PYTHIA [84, 85] and HERWIG/JIMMY [86–88], are described in some detail elsewhere in these proceedings [89]. Common for all these models is that they include exact kinematics and flavour conservation, which introduces some non-trivial effects and makes the multiple scatterings process-dependent. Also, the predictions of the models are very sensitive to the cutoff used to regularize the partonic cross section and to the assumptions made about the distribution of partons in impact parameter space. Nevertheless, the models are quite successful in describing sensitive final-state observables such as multiplicity distributions and jet-pedestal effects [89]. In particular this is true for the model in PYTHIA which has been successfully tuned to Tevatron data[4] by Rick Field [90], the so-called *CDF tune A*.

The PYTHIA model does not make any prediction for the energy dependence of the total cross section - rather this is an input to the model used to obtain the distribution in the number of multiple interactions. PYTHIA can, however, make predictions for gap survival probabilities. This was first done for Higgs production via W-fusion [2], and amounts to simply counting the fraction of events which do not have any additional scatterings besides the W-fusion process. The basic assumption is that any additional partonic scattering would involve a colour exchange which would destroy any rapidity gap introduced by W-fusion process. Since PYTHIA produces complete events, these can also be directly analyzed with the proper experimental cuts. A similar estimate was obtained for the gaps between jets process, both for the Tevatron and HERA case [91].

Recently, PYTHIA was used to estimate gap survival probabilities also for the case of central exclusive Higgs production [92]. As in the case of gaps between jets, the actual signal process is not implemented in PYTHIA, so direct analysis with proper experimental cuts was not possible. Instead a similar hard sub process was used (standard inclusive Higgs production via gluon fusion in this case) and the fraction of events without additional secondary partonic scatterings was identified with the gap survival probability. Using the *CDF tune A* the gap survival probability was estimated to be 0.040 for the Tevatron and 0.026 for the LHC. This is remarkably close both to the values used in [64] obtained in the KKMR model [43], and to the GLM values presented in section 3.4 especially the two-channel ones obtained in [60].

References

[1] Y. L. Dokshitzer, S. I. Troian, and V. A. Khoze, Sov. J. Nucl. Phys. **46**, 712 (1987).

[2] Y. L. Dokshitzer, V. A. Khoze, and T. Sjöstrand, Phys. Lett. **B274**, 116 (1992).

[3] J. D. Bjorken, Int. J. Mod. Phys. **A7**, 4189 (1992).

[4] J. D. Bjorken, Phys. Rev. **D47**, 101 (1993).

[5] D0 Collaboration, S. Abachi *et al.*, Phys. Rev. Lett. **72**, 2332 (1994).

[6] D0 Collaboration, S. Abachi *et al.*, Phys. Rev. Lett. **76**, 734 (1996). `hep-ex/9509013`.

[7] D0 Collaboration, B. Abbott *et al.*, Phys. Lett. **B440**, 189 (1998). `hep-ex/9809016`.

[8] CDF Collaboration, F. Abe *et al.*, Phys. Rev. Lett. **74**, 855 (1995).

[9] CDF Collaboration, F. Abe *et al.*, Phys. Rev. Lett. **80**, 1156 (1998).

[10] CDF Collaboration, F. Abe *et al.*, Phys. Rev. Lett. **81**, 5278 (1998).

[11] CDF Collaboration, T. Affolder *et al.*, Phys. Rev. Lett. **84**, 5043 (2000).

[12] CDF Collaboration, T. Affolder *et al.*, Phys. Rev. Lett. **85**, 4215 (2000).

[13] K. Goulianos (2003). `hep-ph/0306085`.

[14] K. Goulianos, J. Phys. **G26**, 716 (2000). `hep-ph/0001092`.

---

[4]Note that the model in PYTHIA has recently been revised [89]. However, the reproduction of Tevatron data is not as good for the revised model.

[15] CDF Collaboration, K. Goulianos, Nucl. Phys. Proc. Suppl. **99A**, 37 (2001). `hep-ex/0011059`.

[16] K. Goulianos (2004). `hep-ph/0407035`.

[17] K. Goulianos. Private communication to UM.

[18] ZEUS Collaboration, M. Derrick *et al.*, Phys. Lett. **B315**, 481 (1993).

[19] ZEUS Collaboration, M. Derrick *et al.*, Z. Phys. **C68**, 569 (1995). `hep-ex/9505010`.

[20] ZEUS Collaboration, M. Derrick *et al.*, Phys. Lett. **B356**, 129 (1995). `hep-ex/9506009`.

[21] ZEUS Collaboration, M. Derrick *et al.*, Phys. Lett. **B369**, 55 (1996). `hep-ex/9510012`.

[22] ZEUS Collaboration, J. Breitweg *et al.*, Eur. Phys. J. **C6**, 43 (1999). `hep-ex/9807010`.

[23] H1 Collaboration, T. Ahmed *et al.*, Nucl. Phys. **B429**, 477 (1994).

[24] H1 Collaboration, T. Ahmed *et al.*, Phys. Lett. **B348**, 681 (1995). `hep-ex/9503005`.

[25] H1 Collaboration, C. Adloff *et al.*, Z. Phys. **C76**, 613 (1997). `hep-ex/9708016`.

[26] F.-P. Schilling, *Measurement and nlo dglap qcd interpretation of diffractive deep-inelastic scattering at hera.* Paper 089 submitted to EPS 2003 Conf. Aachen.

[27] A. A. Savin. Prepared for NATO Advanced Research Workshop on Diffraction 2002, Alushta, Ukraine, 31 Aug - 6 Sep 2002.

[28] H. Abramowicz, ECONF **C0406271**, MONT04 (2004). `hep-ex/0410002`.

[29] O. Gutsche, *Dijets in diffractive photoproduction and deep-inelastic scattering at hera.* Contribution No. 6-0177 submitted to ICHEP04, Beijing Aug 2004.

[30] E. Gotsman, E. M. Levin, and U. Maor, Z. Phys. **C57**, 677 (1993). `hep-ph/9209218`.

[31] E. Gotsman, E. M. Levin, and U. Maor, Phys. Rev. **D49**, 4321 (1994). `hep-ph/9310257`.

[32] E. Gotsman, E. M. Levin, and U. Maor, Phys. Lett. **B353**, 526 (1995). `hep-ph/9503394`.

[33] E. Gotsman, E. M. Levin, and U. Maor, Phys. Lett. **B347**, 424 (1995). `hep-ph/9407227`.

[34] J. Forshaw, *Diffractive Higgs production: theory.* These Proceedings.

[35] E. Gotsman, E. M. Levin, and U. Maor, Phys. Lett. **B309**, 199 (1993). `hep-ph/9302248`.

[36] E. Gotsman, E. Levin, and U. Maor, Nucl. Phys. **B493**, 354 (1997). `hep-ph/9606280`.

[37] E. Gotsman, E. Levin, and U. Maor, Phys. Lett. **B438**, 229 (1998). `hep-ph/9804404`.

[38] E. Gotsman, E. Levin, and U. Maor, Phys. Lett. **B452**, 387 (1999). `hep-ph/9901416`.

[39] E. Gotsman, E. Levin, and U. Maor, Phys. Rev. **D60**, 094011 (1999). `hep-ph/9902294`.

[40] V. A. Khoze, A. D. Martin, and M. G. Ryskin, Eur. Phys. J. **C14**, 525 (2000). `hep-ph/0002072`.

[41] V. A. Khoze, A. D. Martin, and M. G. Ryskin, Eur. Phys. J. **C18**, 167 (2000). `hep-ph/0007359`.

[42] V. A. Khoze, A. D. Martin, and M. G. Ryskin, Eur. Phys. J. **C19**, 477 (2001). `hep-ph/0011393`.

[43] A. B. Kaidalov, V. A. Khoze, A. D. Martin, and M. G. Ryskin, Eur. Phys. J. **C21**, 521 (2001). `hep-ph/0105145`.

[44] A. B. Kaidalov, V. A. Khoze, A. D. Martin, and M. G. Ryskin, Eur. Phys. J. **C33**, 261 (2004). `hep-ph/0311023`.

[45] P. D. B. Collins, *An Introduction to Regge Theory and High-Energy Physics.* Cambridge 1977, 445p.

[46] L. e. Caneschi, *Current physics sources and comments vol. 3: Regge theory of low p_t hadronic interactions.* North Holland Pub (1989).

[47] A. Donnachie and P. V. Landshoff, Phys. Lett. **B296**, 227 (1992). `hep-ph/9209205`.

[48] A. Donnachie and P. V. Landshoff, Z. Phys. **C61**, 139 (1994). `hep-ph/9305319`.

[49] M. M. Block, K. Kang, and A. R. White, Int. J. Mod. Phys. **A7**, 4449 (1992).

[50] CDF Collaboration, F. Abe *et al.*, Phys. Rev. **D50**, 5535 (1994).

[51] T. T. Chou and C.-N. Yang, Phys. Rev. **170**, 1591 (1968).

[52] S. M. Troshin and N. E. Tyurin, Eur. Phys. J. **C39**, 435 (2005). `hep-ph/0403021`.

[53] A. H. Mueller, Phys. Rev. **D2**, 2963 (1970).

[54] J. Pumplin, Phys. Rev. **D8**, 2899 (1973).

[55] J. Pumplin, Phys. Scripta **25**, 191 (1982).

[56] T. Gitman. TAU M.Sc. Thesis, unpublished (2003).

[57] H1 Collaboration, C. Adloff *et al.*, Phys. Lett. **B483**, 23 (2000). `hep-ex/0003020`.

[58] ZEUS Collaboration, S. Chekanov *et al.*, Eur. Phys. J. **C24**, 345 (2002). `hep-ex/0201043`.

[59] H. Kowalski and D. Teaney, Phys. Rev. **D68**, 114005 (2003). `hep-ph/0304189`.

[60] E. Gotsman, H. Kowalski, E. Levin, U. Maor, and A. Prygarin. Preprint in preparation (2005).

[61] CDF Collaboration, F. Abe *et al.*, Phys. Rev. Lett. **79**, 584 (1997).

[62] A. Donnachie and P. V. Landshoff, Nucl. Phys. **B231**, 189 (1984).

[63] V. A. Khoze, A. D. Martin, and M. G. Ryskin, Phys. Lett. **B401**, 330 (1997). `hep-ph/9701419`.

[64] V. A. Khoze, A. D. Martin, and M. G. Ryskin, Eur. Phys. J. **C23**, 311 (2002). `hep-ph/0111078`.

[65] M. A. Kimber, A. D. Martin, and M. G. Ryskin, Phys. Rev. **D63**, 114027 (2001). `hep-ph/0101348`.

[66] M. A. Kimber, A. D. Martin, and M. G. Ryskin, Eur. Phys. J. **C12**, 655 (2000). `hep-ph/9911379`.

[67] A. G. Shuvaev, K. J. Golec-Biernat, A. D. Martin, and M. G. Ryskin, Phys. Rev. **D60**, 014015 (1999). `hep-ph/9902410`.

[68] A. D. Martin and M. G. Ryskin, Phys. Rev. **D64**, 094017 (2001). `hep-ph/0107149`.

[69] G. Watt, A. D. Martin, and M. G. Ryskin, Eur. Phys. J. **C31**, 73 (2003). `hep-ph/0306169`.

[70] A. B. Kaidalov, V. A. Khoze, A. D. Martin, and M. G. Ryskin, Eur. Phys. J. **C31**, 387 (2003). `hep-ph/0307064`.

[71] V. Khoze. Private communication to UM, July 2005.

[72] M. Arneodo. Talk at HERA/LHC CERN Meeting and private communication to UM, Oct. 2004.

[73] M. M. Block and F. Halzen, Phys. Rev. **D63**, 114004 (2001). `hep-ph/0101022`.

[74] O. J. P. Eboli, E. M. Gregores, and F. Halzen, Phys. Rev. **D61**, 034003 (2000). `hep-ph/9908374`.

[75] O. J. P. Eboli, E. M. Gregores, and F. Halzen, Nucl. Phys. Proc. Suppl. **99A**, 257 (2001).

[76] L. Frankfurt, M. Strikman, and C. Weiss, Annalen Phys. **13**, 665 (2004). `hep-ph/0410307`.

[77] L. Frankfurt, M. Strikman, C. Weiss, and M. Zhalov (2004). `hep-ph/0412260`.

[78] V. A. Petrov and R. A. Ryutin, Eur. Phys. J. **C36**, 509 (2004). `hep-ph/0311024`.

[79] A. Bialas, Acta Phys. Polon. **B33**, 2635 (2002). `hep-ph/0205059`.

[80] A. Bialas and R. Peschanski, Phys. Lett. **B575**, 30 (2003). `hep-ph/0306133`.

[81] M. Klasen and G. Kramer, Eur. Phys. J. **C38**, 93 (2004). `hep-ph/0408203`.

[82] M. Klasen and G. Kramer, Phys. Rev. Lett. **93**, 232002 (2004). `hep-ph/0410105`.

[83] A. B. Kaidalov, V. A. Khoze, A. D. Martin, and M. G. Ryskin, Phys. Lett. **B567**, 61 (2003). `hep-ph/0306134`.

[84] T. Sjöstrand and M. van Zijl, Phys. Rev. **D36**, 2019 (1987).

[85] T. Sjöstrand, and others, Comput. Phys. Commun. **135**, 238 (2001). `hep-ph/0010017`.

[86] G. Corcella *et al.*, JHEP **01**, 010 (2001). `hep-ph/0011363`.

[87] J. M. Butterworth, J. R. Forshaw, and M. H. Seymour, Z. Phys. **C72**, 637 (1996). `hep-ph/9601371`.

[88] J. Butterworth *et al.* `http://jetweb.hep.ucl.ac.uk/JIMMY`.

[89] C. Buttar *et al.*, *Underlying events*. These Proceedings.

[90] R. Field, *Min-bias and the underlying event at the tevatron and the lhc*. `http://www.phys.ufl.edu/~rfield/cdf/FNAL_Workshop_10-4-02.pdf`. Talk presented at the Fermilab ME/MC Tuning Workshop, October 4, 2002.

[91] B. Cox, J. Forshaw, and L. Lönnblad, JHEP **10**, 023 (1999). `hep-ph/9908464`.

[92] L. Lönnblad and M. Sjödahl, JHEP **05**, 038 (2005). `hep-ph/0412111`.